

Supporting Information

© Wiley-VCH 2014

69451 Weinheim, Germany

NMR Fingerprints of the Drug-like Natural-Product Space Identify Iotrochotazine A: A Chemical Probe to Study Parkinson's Disease**

*Tanja Grkovic, Rebecca H. Pouwer, Marie-Laure Vial, Luca Gambini, Alba Noël, John N. A. Hooper, Stephen A. Wood, George D. Mellick, and Ronald J. Quinn**

anie_201402239_sm_miscellaneous_information.pdf

Table of contents:

S1	Experimental section	S2
Table S1	NMR data for ietrochotazine A (1) in [D ₆]DMSO	S5
S2	Synthesis of ietrochotazine A	S5
Scheme S1	Synthesis of ietrochotazine A	S5
S3	Cell assays	S6
S4	Structural elucidation of ietrochotadines A – D (2 – 5)	S8
Figure S1	Crucial 2D NMR correlations used to establish the structure of 2 .	S9
Table S2	NMR data for ietrochotadines A (2) and C (4) in [D ₆]DMSO	S9
Figure S2	A comparison of ¹ H NMR spectra of <i>Ietrochota</i> sp. LLE extract	S12
Figure S3	<i>Ietrochota</i> sp. LLE fractions 1 -5 ¹ H NMR fingerprint summary	S13
Figure S4	Biological activity profile of ietrochotazine A – PD phenotypic panel	S14
Figure S5	¹ H NMR spectrum of naturally-occurring ietrochotazine A (1) in [D ₆]DMSO	S15
Figure S6	¹³ C NMR spectrum of naturally-occurring ietrochotazine A (1) in [D ₆]DMSO	S16
Figure S7	Edited ¹ H- ¹³ C HSQC NMR spectrum of naturally-occurring ietrochotazine A (1) in [D ₆]DMSO	S17
Figure S8	¹ H- ¹³ C HMBC NMR spectrum of naturally-occurring ietrochotazine A (1) in [D ₆]DMSO	S18
Figure S9	¹ H NMR spectrum of ietrochotadine A trifluoroacetate salt (2) in [D ₆]DMSO	S19
Figure S10	¹³ C NMR spectrum of ietrochotadine A trifluoroacetate salt (2) in [D ₆]DMSO	S20
Figure S11	Edited ¹ H- ¹³ C HSQC NMR spectrum of ietrochotadine A trifluoroacetate salt (2) in [D ₆]DMSO	S21
Figure S12	¹ H- ¹³ C HMBC NMR spectrum of ietrochotadine A trifluoroacetate salt (2) in [D ₆]DMSO	S22
Figure S13	¹ H NMR spectrum of ietrochotadine B trifluoroacetate salt (3) in [D ₆]DMSO	S23
Figure S14	¹³ C NMR spectrum of ietrochotadine B trifluoroacetate salt (3) in [D ₆]DMSO	S24
Figure S15	¹ H NMR spectrum of ietrochotadine C trifluoroacetate salt (4) in [D ₆]DMSO	S25
Figure S16	¹³ C NMR spectrum of ietrochotadine C trifluoroacetate salt (4) in [D ₆]DMSO	S26
Figure S17	¹ H NMR spectrum of ietrochotadine D trifluoroacetate salt (5) in [D ₆]DMSO	S27
Figure S18	Edited ¹ H- ¹³ C HSQC NMR spectrum of ietrochotadine D trifluoroacetate salt (5) in [D ₆]DMSO	S28
Figure S19	¹ H- ¹³ C HMBC NMR spectrum of ietrochotadine D trifluoroacetate salt (5) in [D ₆]DMSO	S29
Figure S20	¹ H NMR spectral comparison of naturally-occurring 1 and synthetic 1 in [D ₆]DMSO	S30
Figure S21	¹³ C NMR spectral comparison of naturally-occurring 1 and synthetic 1 in [D ₆]DMSO	S31
Figure S22	Pototograph of the sponge <i>Ietrochota</i> sp. QM2256	S32
References		S33

S1 Experimental Section

General Methods. UV spectra were recorded on a Jasco V650 UV/vis spectrophotometer. NMR spectra were recorded at 30 °C on either a Varian 500 or 600 MHz Unity INOVA spectrometer. The latter spectrometer was equipped with a triple resonance cold probe. The ^1H and ^{13}C NMR chemical shifts were referenced to the solvent peaks for $[\text{D}_6]\text{DMSO}$ at δ_{H} 2.50 and δ_{C} 39.45, respectively. LR-ESIMS were recorded on a Waters ZQ single quadrupole ESI spectrometer or on an Agilent 6120 quadrupole LCMS system. HRESIMS were recorded on a Bruker Daltonics Apex III 4.7e Fourier-transform mass spectrometer. Waters Oasis HLB (400 mg) solid-phase extraction cartridge was used to purify the small-scale sponge extracts. Pre-fractionation was performed on a Phenomenex Onyx Monolythic C_{18} column [100 x 4.6 mm]. A BIOLINE orbital shaker was used for the large-scale extraction of sponge material. A Waters LCMS system equipped with Phenomenex Onyx Monolythic C_{18} column [100 x 2.0 mm], a PDA detector, a ZQ ESI mass spectrometer and an ELSD detector was used for the fractionation work. A Waters 600 pump equipped with a Waters 996 PDA detector and a Waters 717 autosampler were used for HPLC. A Thermo-Electron C_{18} Betasil 143 Å column [5 μm , 150 x 21.2 mm] or a BDS Hypersil C_8 column [5 μm , 250 x 10 mm] were used for semi-preparative HPLC separations. All solvents used for chromatography, UV, and MS were Lab-Scan HPLC grade (RCI Lab-Scan, Bangkok, Thailand), and the H_2O was Millipore Milli-Q PF filtered.

LLE fraction library generation. Each LLE extract was fractionated into 11 LLE fractions which were used for ^1H NMR analysis. The extraction and lead-like fraction library generation have been conducted as previously described.¹

Metabolic fingerprinting methodology. Four combined replicates of each of the 11 LLE fractions were analysed by ^1H NMR. The samples were dissolved in 200 μL of $[\text{D}_6]\text{DMSO}$ and run in a 3 mm NMR tube. The standard VnmrJ 3.2 Proton pulse sequence was run with the following parameters: $\text{pw} = 45^\circ$, $\text{p1} = 0 \mu\text{s}$, $\text{d2} = 0 \text{ s}$, $\text{d1} = 1 \text{ s}$, $\text{at} = 1.7 \text{ s}$, $\text{sw} = 9615\text{Hz}$, $\text{nt} = 128$ scans.

Animal Material. The sponge *Iotrochota* sp. QM2256 (Phylum Porifera, class Demospongiae, order Poecilosclerida, suborder Myxillina, family Iotrochotidae) was collected at Low Isles, Great Barrier Reef, Queensland, Australia by SCUBA at a depth of 24m in January, 1997. The material was kept freeze-dried prior to extraction. A voucher specimen (QMG307894) is deposited at the Queensland Museum, Brisbane, Australia. The sponge displays an arborescent form and simple branching, with cylindrical digitate branches and few bifurcations. The surface is highly convoluted and rugged. The animal is dark purple alive and dark purple in ethanol. There are no visible oscules, and the texture is firm, harsh and incompressible. The ectosomal skeleton is membranous with a thin unispicular layer of strongyles in confused reticulation. The choanosomal skeleton is regular, densely packed, multispicular tracts of strongyles with individual strongyles scattered in between. Tracts of strongyles are not bound by spongin. Mesohyl collagen is moderately light but highly collagenous and is pigmented dark red. Megasclere details include strongyles (150 μm) and styles (220 μm). Microsclere details include styles (142 μm).

Large-scale Extraction and Isolation. Freeze-dried *Iotrochota* sp. sponge (10.0 g) was sequentially extracted with *n*-hexane (250 mL), CH_2Cl_2 (250 mL) and MeOH (2 \times 250 mL). The CH_2Cl_2 and MeOH extracts were combined and dried under reduced pressure to yield a dark brown oil (1.20 g). The sponge crude extract was then loaded on a C_8 flash column and de-salted eluting with MeOH/ H_2O (1:9) (200 mL), followed by a MeOH/ H_2O (9:1) (200 mL) wash to yield 178 mg of salt- and fatty acid-free

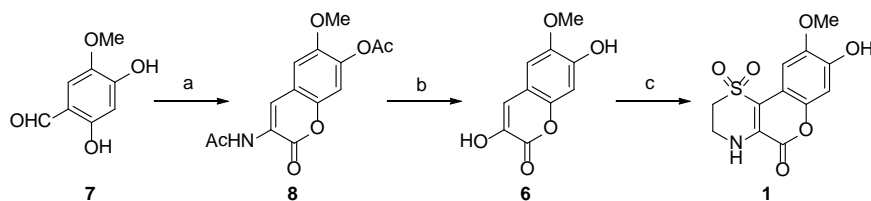
crude extract. The semi-purified crude extract was pre-adsorbed to C₁₈-bonded silica, and then packed into a stainless steel HPLC guard cartridge (10 × 30 mm) that was subsequently attached to a C₁₈ Betasil HPLC column. Isocratic HPLC conditions of 90% H₂O (0.1% TFA)/10% MeOH (0.1% TFA) were initially employed for 10 min, then a linear gradient to MeOH (0.1% TFA) was run over 40 min, followed by isocratic conditions of MeOH (0.1% TFA) for a further 10 min, all at a flow rate of 9 mL/min. Sixty fractions (60 × 1 min) were collected from time = 0 min, and then analyzed by (+)-LR-ESIMS. Fraction 21 yielded 0.2 mg of **5** (0.002% dry wt), fraction 23 yielded 0.4 mg of **4** (0.004% dry wt), fraction 28 yielded 0.9 mg of **3** (0.009% dry wt) and fraction 29 yielded 1.6 mg of **2** (0.016% dry wt). Combined fractions 30 and 31 were further purified by semi-preparative HPLC using a BDS Hypersil C₈ column [250 × 10 mm] eluting with a gradient from H₂O (0.1% TFA) / MeOH (0.1% TFA) (80:20 to 30:70 over 30 min) to yield **1** (2.5 mg, 0.025% dry weight).

Iotrochotazine A (1): yellow oil; $[\alpha]_D = 0$ (*c* 0.1, MeOH); UV (MeOH) λ_{\max} (log ϵ) 212 (4.29), 249 (3.84), 287 (3.46), 371 (3.79) nm; IR (smear) ν_{\max} 2924, 1686, 1560, 1383, 1210 cm⁻¹; ¹H NMR ([D₆]DMSO, 600 MHz) and ¹³C NMR ([D₆]DMSO, 125 MHz) data, see Table S1; HRESIFTMS *m/z* [M+Na]⁺ 320.020562 (calcd for C₁₂H₁₁NO₆SNa, 320.019929).

no	δ_C (mult)	δ_H (mult <i>J</i> in Hz)	HMBC ^a
2	48.4 (CH ₂)	3.55 (m)	3,10b
3	38.8 (CH ₂)	3.80 (m)	2,4a
4		7.56 (br t, 3.1)	2,3,4a,5,10b
4a	129.9 (C)		
5	156.8 (C)		
6a	140.7 (C)		
7	103.6 (CH)	6.79 (s)	6a,8,9,10a,10b
8	145.9 (C)		
9	145.2 (C)		
10	105.0 (CH)	7.42 (s)	6a,7,8,9,10a,10b
10a	105.9 (C)		
10b	112.1 (C)		
9-OMe	56.0 (CH ₃)	3.77 (s)	9
8-OH		9.74 (s)	7,9

Table S1. NMR data for iotrochotazine A (**1**) in [D₆]DMSO
^aHMBC correlations, optimized for 8.0 Hz are from proton(s) stated to the indicated carbon.

S2 Synthesis of iotrochotazine A



Scheme S1. Synthesis of Iotrochotazine A

Synthesis of 3-Acetamido-6-methoxy-7-acetoxycoumarin (8) A stirred solution of 2,4-dihydroxy-5-methoxybenzaldehyde² (540 mg, 3.9 mmol), *N*-acetylglycine (687 mg, 5.8 mmol), and anhydrous sodium acetate (385 mg, 4.7 mmol) in acetic anhydride (3 mL) was heated to 140 °C for 3 h. The reaction mixture was cooled to RT, and ice (20 g) was added. The mixture was stirred for 14 h, after which time the resulting brown precipitate was collected by filtration. The crude material was suspended in hot ethanol and filtered to yield the title compound **8** (280 mg, 25%) as a light brown powder. m.p. >250 °C; ¹H NMR (500 MHz, CDCl₃) δ 8.64 (s, 1H), 8.06

(s, 1H), 7.07 (s, 1H), 7.00 (s, 1H), 3.87 (s, 3H), 2.34 (s, 3H), 2.24 (s, 3H) ppm; ^{13}C NMR (125 MHz, CDCl_3) δ 169.4, 168.5, 158.5, 149.0, 143.7, 141.1, 123.9, 122.7, 118.0, 111.5, 109.3, 56.4, 24.7, 20.6 ppm; LCMS (ESI) 314 ($\text{M} + \text{Na}$) $^+$, 292 ($\text{M} + \text{H}$) $^+$.

Synthesis of 3,7-Dihydroxy-6-methoxycoumarin (6) A stirred solution of **8** (230 mg, 0.79 mmol) in 3 M HCl (aq) (7.5 mL) and acetic acid (7.5 mL) was heated to 130 °C for 16 h. The solution was cooled to RT, and the solvent was removed in vacuo. The residue was dissolved in 1:1 dichloromethane/acetone, pre-loaded on to silica, and purified by silica gel column chromatography (dichloromethane to 4:1 dichloromethane/acetone) to yield the title compound **6** (96 mg, 59%) as a yellow powder. Spectra was identical to that previously reported for this compound.³

Synthesis of Iotrochotazine A (1). To a stirred solution of **6** (10 mg, 0.05 mmol) in CH_3CN (0.5 mL) and EtOH (0.5 mL) and H_2O (0.5 mL) was added hypotaurine (12 mg, 0.11 mmol). The solution was bubbled with oxygen gas, and then heated to 80°C under an atmosphere of oxygen for 2 days. A further portion of hypotaurine (12 mg, 0.11 mmol) was added, and heating was continued for a further 4 days until **6** was consumed (monitored by LCMS). The reaction mixture was cooled to RT, and the solvent was removed in vacuo. The residue was dissolved in 1:1 *n*-butanol/dichloromethane (50 mL) and washed with H_2O (2 x 10 mL). The organic phase was concentrated in vacuo to yield the title compound (10 mg, 70%) as a light brown powder. Spectra were identical to that found for the isolated material.

S3 Cell assays

Compound transfer. 10 nL of iotrochotazine A filled to 300 nL with DMSO were automatically transferred into 2 optically clear bottom CellCarrier™ 384-well plates (PerkinElmer). hONS cells from PD patient (cell line #2813) and healthy individuals

(#1817 and #1901) were added to compounds at a density of 1,350 cells per well in 50 μ L of growth medium (DMEM/F12, 10% FBS) leading to a final concentration of 1 μ M, 0.6% DMSO. 0.6% DMSO was used as negative control to determine baseline response. The cells were incubated for 24 h at 37°C in a 5% CO₂ humidified incubator.

Cell staining. After 24 h of incubation with the compound, one 384-well plate was treated with 400 nM MitoTracker® Orange CMTMRos (Invitrogen) for 30 min at 37°C, 5% CO₂. The second 384-well plate was treated with 100 nM LysoTracker® Red DND-99 (Invitrogen) for 1 h at 37°C, 5% CO₂. Cells were fixed in 4% paraformaldehyde for 5 min at room temperature (RT). Cells were washed twice with phosphate-buffered saline (PBS, Sigma-Aldrich) and treated with 3% goat serum (Sigma-Aldrich) and 0.2% Triton X-100 (Sigma-Aldrich) in PBS for 45 min at RT. Plates were incubated with primary antibodies. Mouse anti- α -tubulin (Sigma-Aldrich) and rabbit anti-LC3b (Sigma-Aldrich) were added to the plate already treated with MitoTracker®. Mouse anti-EEA1 (Sigma-Aldrich) was added to the plate treated with LysoTracker®. Plates were incubated at RT for 1 h then washed twice with PBS. Secondary antibodies, goat anti-mouse Alexa-647 1/500 (Invitrogen) and goat anti-rabbit Alexa-488 1/500 (Invitrogen) were added to the first plate and goat anti-mouse Alexa-488 1/500 (Invitrogen) was added to the second plate for 30 min at RT. Cells were washed twice with PBS and stained with 4',6'-diamidino-2-phenylindole 1/5000 (Dapi, Invitrogen) and with CellMask™ Deep Red 1/5000 (Invitrogen) for the plate treated with LysoTracker® and incubated for 10 min at RT. Cells were washed twice with PBS and plates were stored in the dark at 4 °C with 25 μ L of PBS/well.

Imaging and image analysis. Plates were imaged automatically using Operetta™ (PerkinElmer), a high content imaging system using a 20X high numerical aperture

objective lens. 6 images per well for each wavelength were collected. Individual cell segmentation was done using the Harmony® software and measurements for each cell were performed generating 38 parameters from 6 dyes: Dapi, α -tubulin staining, MitoTracker® Orange CMTMRos, LC3b staining, LysoTracker® Red DND-99 and EEA1 staining. The normality of the data was checked for each parameter and a log2 transformation was made when required. The measurements were then converted to a score.

S4 Structural elucidation of iotrochotadines A – D (2 – 5)

Iochotadine A (**2**) was isolated as an optically inactive clear oil with a molecular formula of $C_{14}H_{22}N_4O$ established by HR-ESI-FT-MS, which required five double bond equivalents. Interpretation of the 1H and ^{13}C NMR data (Table S2) allowed for the identification of the elements of unsaturation to be: a monosubstituted phenyl group (δ_H 7.21 1H, m; 7.24 2H, m; 7.29 2H, m; δ_C 136.5, C; 128.9, 2CH; 128.2, 2CH; 126.2, CH), an imine (δ_C 156.6) and a carbonyl (δ_C 169.9). The remaining resonances were: two exchangeable broad triplets (δ_H 8.01, $J = 5.0$ Hz; 7.49, $J = 5.1$ Hz), a methylene singlet (δ_H 3.38; δ_C 42.4) and five other sp^3 hybridized methylenes (δ_H 3.05, m, δ_C 40.6; δ_H 3.03, m, δ_C 38.4; δ_H 1.45, m, δ_C 28.0; δ_H 1.41, m, δ_C 28.7; δ_H 1.25, m, δ_C 23.4). Starting from an exchangeable NH proton at δ_H 8.01, 2D COSY and HMBC correlations were used to assign the 1-(5-aminopentyl) guanidine partial structure. An HMBC correlation from H6' to an imine carbon at δ_C 156.6 depicted in Figure S1, confirmed the connectivity between the aminopentyl chain and the terminal guanidine group. Comparison of the spectroscopic data with the known natural products that contain a similar amino alkyl guanidine moiety,^{4,5} confirmed the structural assignment of this fragment. The methylene singlet resonance at δ_H 3.38 showed HMBC correlations to both the phenyl ring carbons and a carbonyl resonance and was assigned to a benzylic position alpha to a carbonyl group, with the

spectroscopic data in close agreement with other natural products that contain the phenyl acetyl moiety.^{6,7} The connectivity between the two partial substructures was established via HMBC correlations between NH1' and H2' methylenes to the carbonyl at C1 to complete the structure of iotochotadine A (**2**).

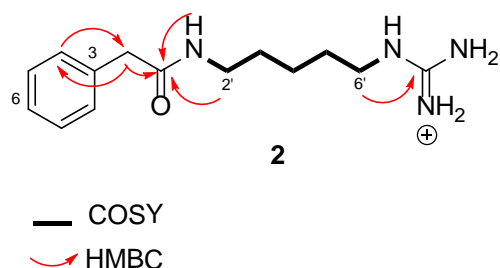


Figure S1. Crucial 2D NMR correlations used to establish the structure of **2**.

The HR-ESI-FT-MS spectrum of iotochotadine B (**3**), showed a loss of 14 amu compared to that of **2**. A comparison of the ¹H and ¹³C spectroscopic data showed the only significant difference to be the loss of a methylene group, consistent with the molecular formula of C₁₃H₂₀N₄O. Compound **3** was therefore concluded to be the 1-(4-aminobutyl) guanidine analogue of **2**.

2				4			
no	δ_C^a (mult)	δ_H (mult <i>J</i> in Hz)	HMBC ^b	no	δ_C^a (mult)	δ_H (mult <i>J</i> in Hz)	HMBC ^b
1	169.9 (C)			1	170.3 (C)		
2	42.4 (CH ₂)	3.38 (s)	1,3,4	2	41.5 (CH ₂)	3.24 (s)	1,3,4
3	136.5 (C)			3	126.5 (C)		2,6
4	128.9 (CH)	7.24 (m)	6	4	129.7 (CH)	7.02 (d, 8.3)	3,6
5	128.2 (CH)	7.29 (m)	3	5	114.8 (CH)	6.67 (d, 8.3)	
6	126.2 (CH)	7.21 (m)	4	6	155.7 (C)		
1'		8.01 (br t, 5.0)	1,2'	1'		7.88 (br t, 5.2)	1
2'	38.4 (CH ₂)	3.03 (m)	1,4'	2'	38.3 (CH ₂)	3.02 (dd, 13.1, 6.9)	1,3',4'
3'	28.7 (CH ₂)	1.41 (m)	2',4',5'	3'	28.6 (CH ₂)	1.38 (m)	2',4',5'
4'	23.4 (CH ₂)	1.25 (m)	2',3',5',6'	4'	23.3 (CH ₂)	1.25 (m)	2',3',5',6'
5'	28.0 (CH ₂)	1.45 (m)	3',4',6'	5'	27.9 (CH ₂)	1.45 (m)	3',4',6'
6'	40.6 (CH ₂)	3.05 (m)	4',8'	6'	40.5 (CH ₂)	3.05 (dd, 13.2, 6.8)	4',5',8'
7'		7.49 (br t, 5.1)		7'		7.48 (br t, 5.2)	
8'	156.6 (C)			8'	156.5 (C)		
9'		not observed		9'		not observed	
				6-OH		9.19 (s)	5,6

Table S2. NMR data for iotochotadines A (**2**) and C (**4**) in [D₆]DMSO
^aHMBC correlations, optimized for 8.0 Hz are from proton(s) stated to the indicated carbon.

Iotrochotadine C (**4**), with the molecular formula of $C_{14}H_{22}N_4O_2$ determined by HR-ESI-FT-MS, had an extra oxygen atom compared to **2** but calculated for the same number of double bond equivalents. A comparison of the 1H and ^{13}C spectroscopic data revealed that **4** had an identical aminopentyl guanidine chain to that of **2**, with the major differences centered on the benzene ring resonances (Table S2). The narrow aromatic multiplet band in **2** was replaced with two mutually coupled doublets (δ_H 7.02, 2H, d, $J = 8.3$ Hz, δ_C 129.7; δ_H 6.67, 2H, d, $J = 8.3$ Hz, δ_C 114.8) and a broad exchangeable singlet (δ_H 9.19), consistent with a *para*-substituted phenol substituent. The structure of iotrochotadine C (**4**) was therefore established to be the 6-phenol analogue of **2**. The HR-ESI-FT-MS spectrum of iotrochotadine D (**5**), showed a loss of 14 amu compared to that of **4**. A comparison of the 1H spectroscopic data for **5** with that of **4**, revealed a loss of a contiguous methylene group. 2D NMR data confirmed the structure of iotrochotadine D (**5**) to be the 1-(4-aminobutyl) guanidine chain analogue of **4**.

Iotrochotadine A (2): clear oil; $[\alpha]_D = 0$ (c 0.1, MeOH); UV (MeOH) λ_{max} (log ϵ) 202 (4.02), 253 (3.08) nm; IR (smear) ν_{max} 2925, 2852, 1659, 1642, 1384, 1204, 1138 cm^{-1} ; 1H NMR ($[D_6]$ DMSO, 600 MHz) and ^{13}C NMR ($[D_6]$ DMSO, 150 MHz) data, see Table 2; HRESIFTMS m/z $[M+H]^+$ 263.186603 (calcd for $C_{14}H_{23}N_4O$, 263.186638).

Iotrochotadine B (3): clear oil; $[\alpha]_D = 0$ (c 0.1, MeOH); UV (MeOH) λ_{max} (log ϵ) 202 (4.02), 255 (2.89) nm; IR (smear) ν_{max} 3347, 2927, 2342, 1659, 1549, 1384, 1203, 1136 cm^{-1} ; 1H NMR ($[D_6]$ DMSO, 600 MHz) δ 8.09 (1H, t, $J = 5.4$ Hz, H-1'), 7.50 (1H, t, $J = 5.0$ Hz, H-6'), 7.27 (2H, m, H-5), 7.22 (2H, m, H-4), 7.19 (1H, m, H-6), 3.39 (2H, s, H-2), 3.08 (2H, dd, $J = 12.2, 6.2$ Hz, H-5'), 3.05 (2H, dd, $J = 12.1, 6.2$ Hz, H-2'), 1.42 (4H, m, H-3'/4'); ^{13}C NMR ($[D_6]$ DMSO, 150 MHz) δ 170.0 (C-1),

156.6 (C-9'), 136.5 (C-3), 128.9 (C-4), 128.2 (C-5), 126.3 (C-6), 42.4 (C-2), 40.4 (C-5'), 38.1 (C-2'), 26.3 (C-3'), 25.9 (C-4'); HRESIFTMS m/z $[M+Na]^+$ 271.151806 (calcd for $C_{13}H_{20}N_4ONa$, 271.152932).

Iotrochotadine C (4): clear oil; $[\alpha]_D = 0$ (c 0.1, MeOH); UV (MeOH) λ_{max} ($\log \epsilon$) 202 (4.19), 225 sh (3.89), 275 (3.35), 285 (3.32) nm; 1H NMR ($[D_6]$ DMSO, 600 MHz) and ^{13}C NMR ($[D_6]$ DMSO, 150 MHz) data, see Table 2; HRESIFTMS m/z $[M+H]^+$ 279.180177 (calcd for $C_{14}H_{23}N_4O_2$, 279.181552).

Iotrochotadine D (5): clear oil; $[\alpha]_D = 0$ (c 0.1, MeOH); UV (MeOH) λ_{max} ($\log \epsilon$) 202 (4.14), 227 sh (3.87), 276 (3.37), 285 (3.34) nm; 1H NMR ($[D_6]$ DMSO, 600 MHz) δ 9.19 (1H, s, OH-6), 7.92 (1H, t, $J = 5.8$ Hz, H-1'), 7.41 (1H, t, $J = 5.8$ Hz, H-6'), 7.02 (2H, d, $J = 8.5$ Hz, H-4), 6.67 (2H, d, $J = 8.5$ Hz, H-5), 3.25 (2H, s, H-2), 3.08 (2H, dd, $J = 12.4, 6.3$ Hz, H-5'), 3.04 (2H, dd, $J = 12.6, 6.6$ Hz, H-2'), 1.41 (4H, m, H-3'/4'); ^{13}C NMR ($[D_6]$ DMSO, 150 MHz, values measured from HSQC and HMBC experiments) δ 170.4 (C-1), 156.3 (C-9'), 155.4 (C-6), 129.5 (C-4), 126.3 (C-3), 114.4 (C-5), 41.1 (C-2), 40.0 (C-5'), 37.7 (C-2'), 25.9 (C-3'), 25.6 (C-4'); HRESIFTMS m/z $[M+H]^+$ 265.165749 (calcd for $C_{13}H_{21}N_4O_2$, 265.165902).

Figure S2. A comparison of ^1H NMR spectra of *Ietrochota* sp. LLE extract and a single fraction generated from the same biota. The top spectrum shows the crude extract whereas the bottom spectrum is that of a single fraction (LLEF-4). The extended regions A and B clearly demonstrate that while the crude extract spectra are dominated by the major compounds, the fraction spectra are far less complicated and allow the minor metabolites to be distinguished.

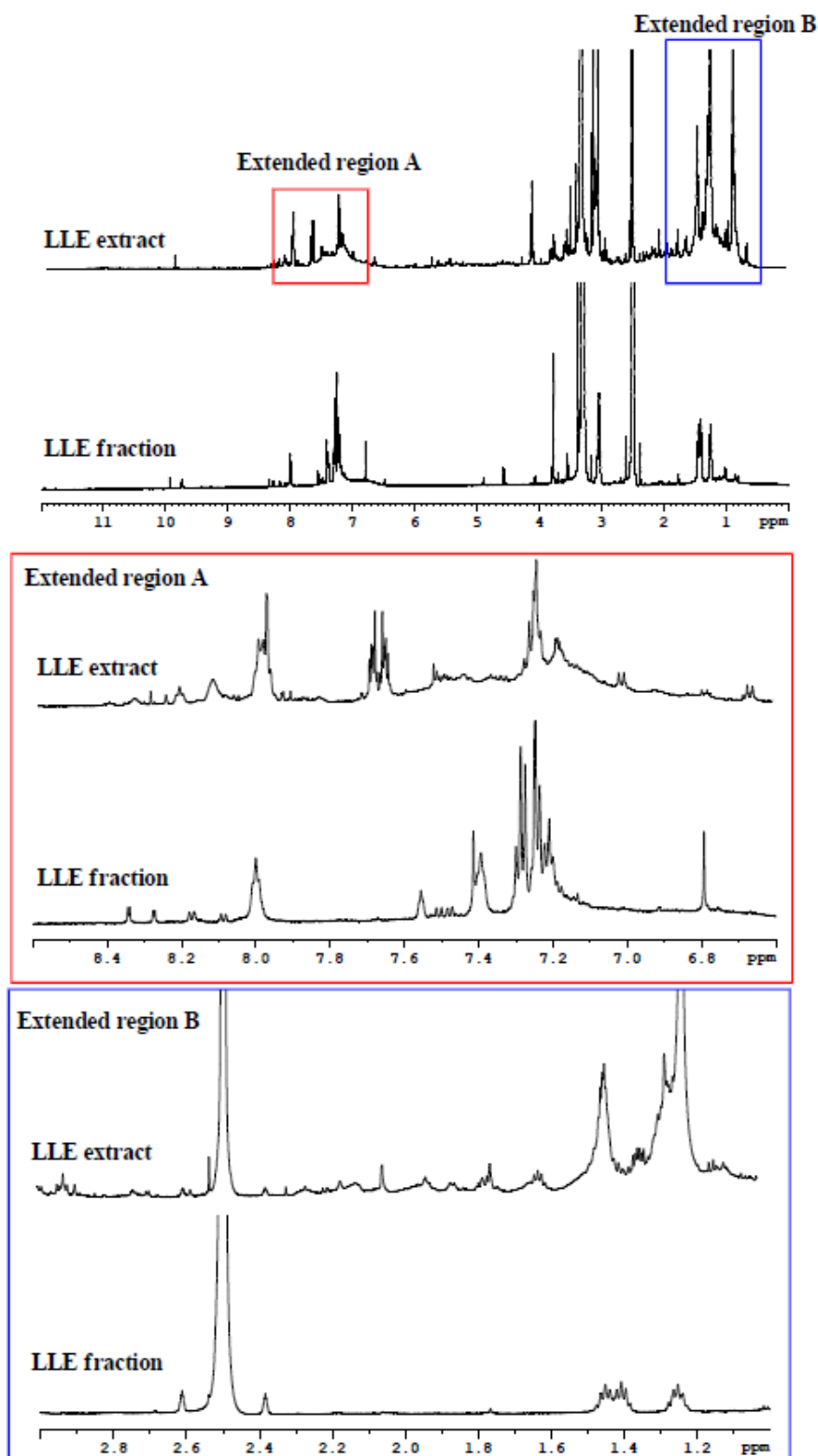


Figure S3. *Iotrochota* sp. LLE fractions 1 -5 ^1H NMR summary. The ^1H NMR spectra represent four combined replicates acquired over 128 scans. The mass ions represent the most abundant m/z values in the LCMS spectrum of each fraction.

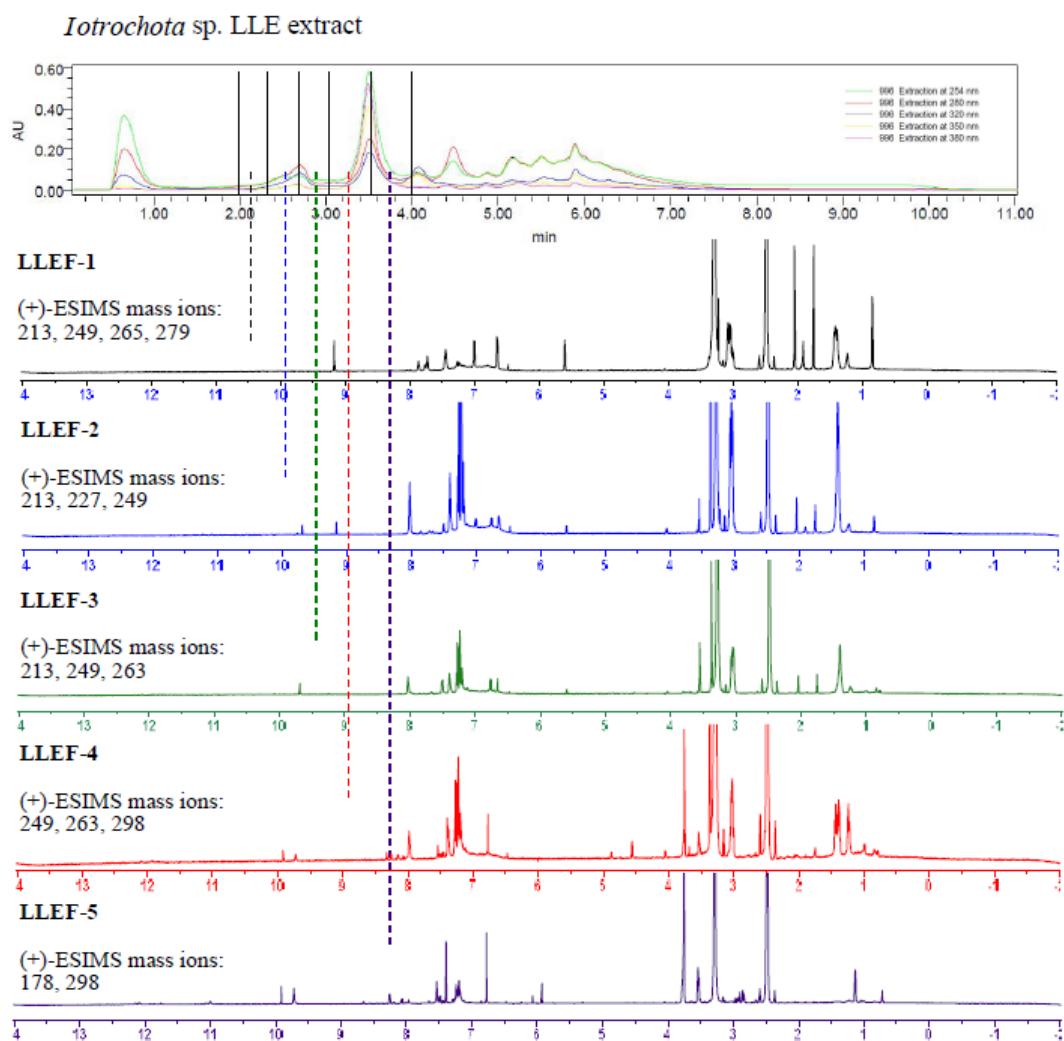
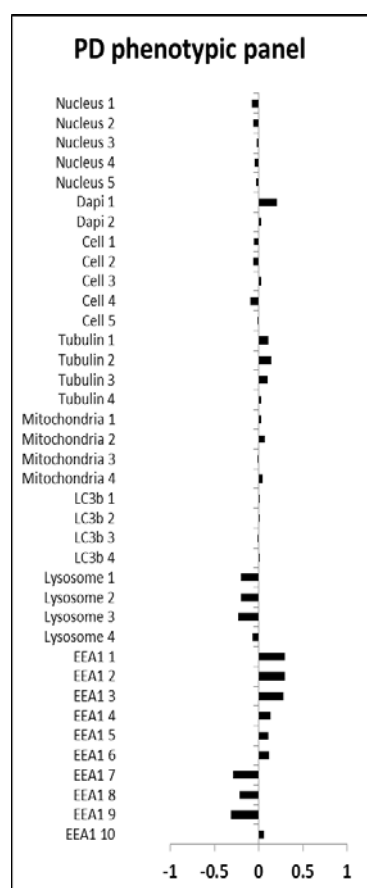


Figure S4. Biological activity profile of iotrochotazine A



hONS-derived Parkinson's disease panel, tested at a single dose of 1 μ M. The data is presented as the log 2 ratio of treatment versus the vehicle control. Legend: Nucleus 1 - nucleus area (μm^2), Nucleus 2 - nucleus width (μm), Nucleus 3 - Nucleus length (μm), Nucleus 4 - nucleus ratio width to length, Nucleus 5- nucleus roundness, Dapi 1 - Dapi marker texture, Dapi 2 - Dapi marker intensity, Cell 1 - cell area (μm^2), Cell 2 - cell width (μm), Cell 3 - cell length (μm), Cell 4 - cell ratio width to length, Cell 5 - cell roundness, Tubulin 1 - tubulin marker intensity in cytoplasm, Tubulin 2 - tubulin marker intensity in outer region of cytoplasm, Tubulin 3 - tubulin marker intensity in inner region of cytoplasm, Tubulin 4 - tubulin marker texture, Mitochondria 1 - mitochondria marker intensity in cytoplasm, Mitochondria 2 - mitochondria marker intensity in outer region of cytoplasm, Mitochondria 3 - mitochondria marker intensity in inner region of cytoplasm, Mitochondria 4 - mitochondria marker texture, LC3b 1 - LC3b marker intensity in cytoplasm, LC3b 2 - LC3b marker intensity in outer region of cytoplasm, LC3b 3 - LC3b marker intensity in inner region of cytoplasm, LC3b 4 - LC3b marker texture, Lysosome 1 - lysosome marker intensity in cytoplasm, Lysosome 2 - lysosome marker intensity in outer region of cytoplasm, Lysosome 3 - lysosome marker intensity in inner region of cytoplasm, Lysosome 4 - lysosome marker texture, EEA1 1 - number of EEA1 spots in cytoplasm, EEA1 2 - number of EEA1 spots in inner region of cytoplasm, EEA1 3 - number of EEA1 spots in outer region of cytoplasm, EEA1 4 - number of EEA1 spots per area of cytoplasm, EEA1 5 - number of EEA1 marker spots per area of outer region, EEA1 6 - number of EEA1 marker spots per area of inner region, EEA1 7 - EEA1 marker spot signal in cytoplasm, EEA1 8 - EEA1 marker spot signal in outer region of cytoplasm, EEA1 9 - EEA1 marker spot signal in inner region of cytoplasm, EEA1 10 - EEA1 marker texture.

Figure S5. ^1H NMR spectrum of naturally-occurring iotrochotazine A (**1**) in $[\text{D}_6]\text{DMSO}$

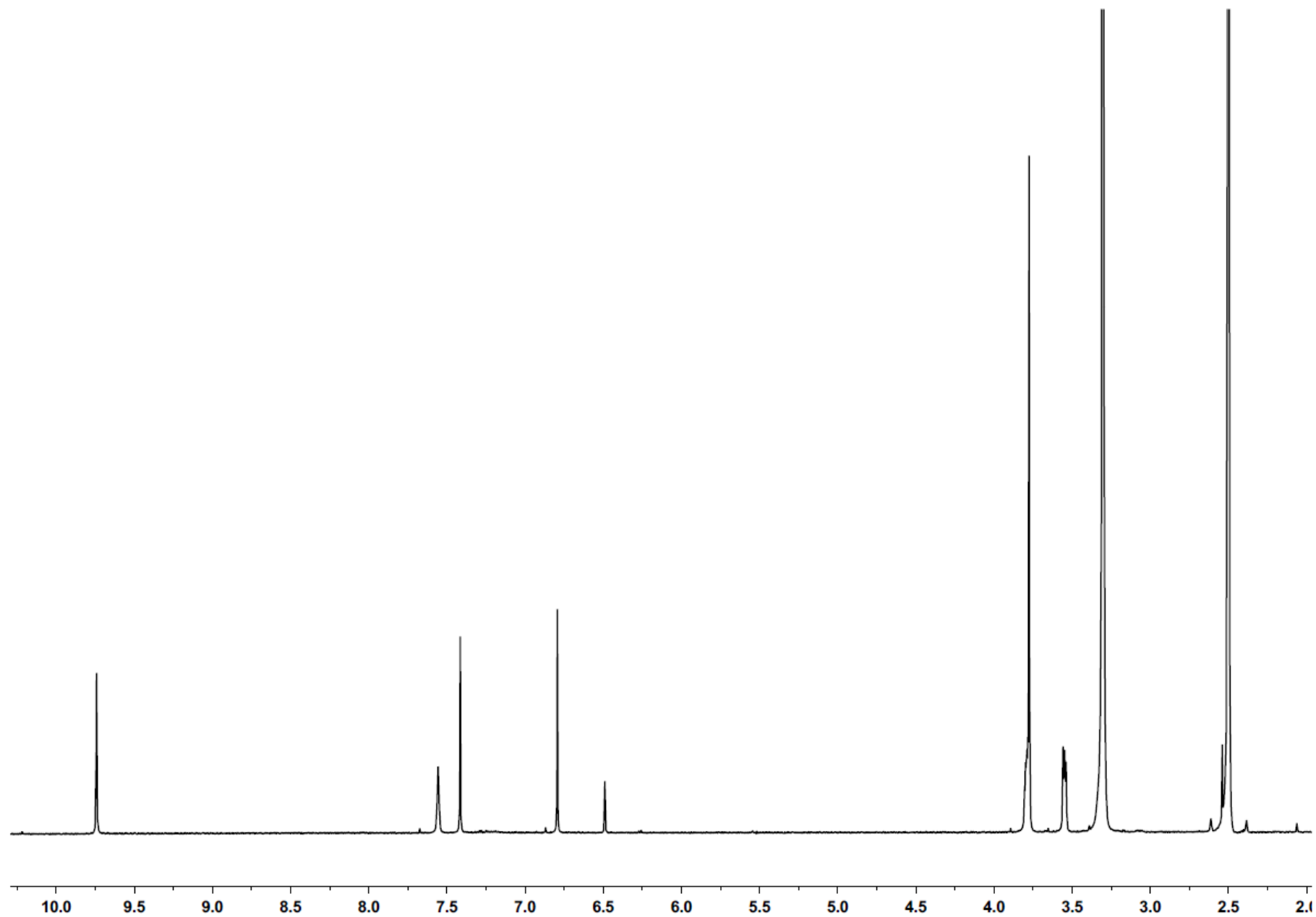


Figure S6. ^{13}C NMR spectrum of naturally-occurring ietrochotazine A (**1**) in $[\text{D}_6]\text{DMSO}$

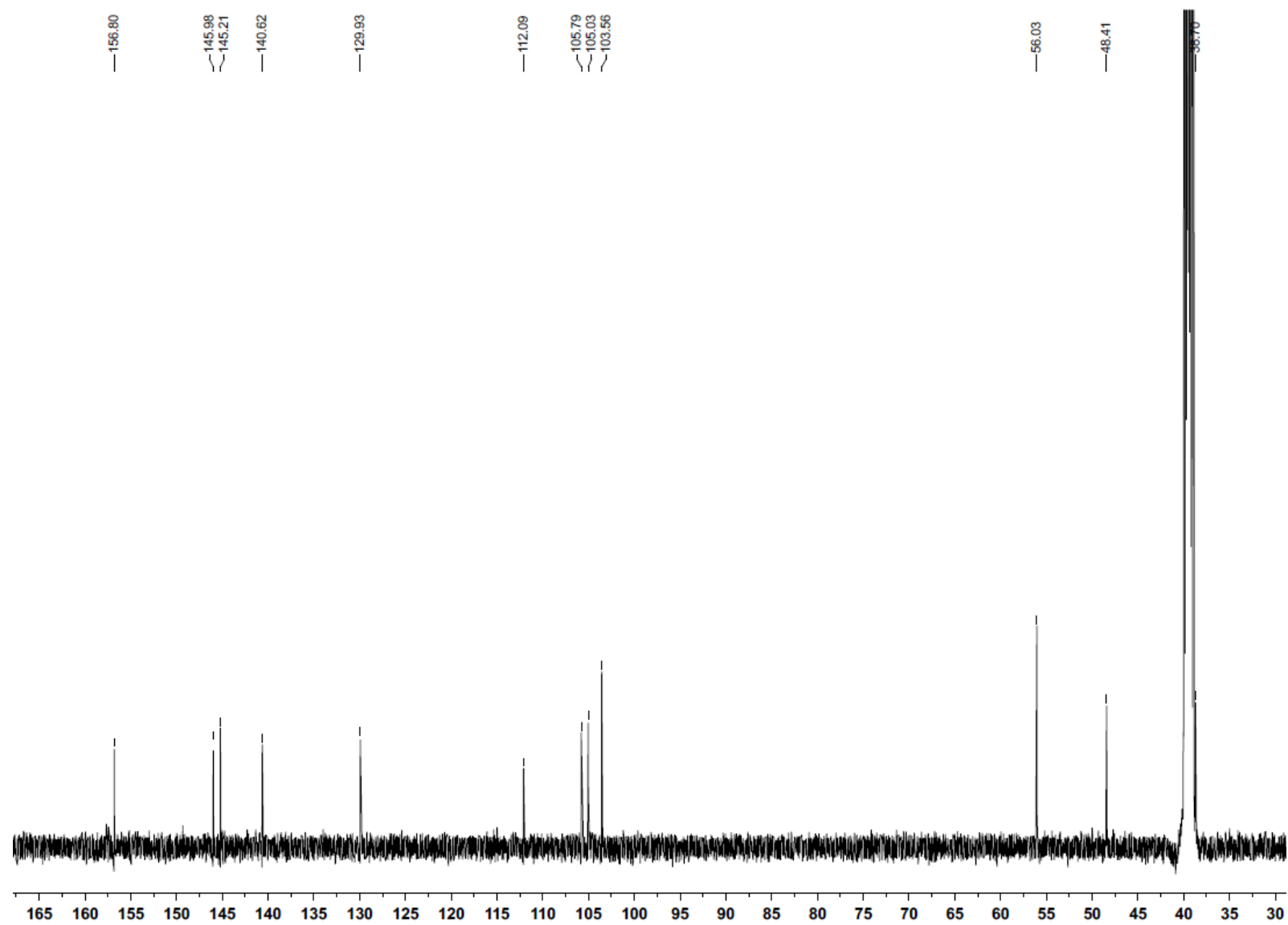


Figure S7. Edited ^1H - ^{13}C HSQC NMR spectrum of naturally-occurring iotrochotazine A (**1**) in $[\text{D}_6]\text{DMSO}$. The decoupler was turned off during acquisition resulting in signals being split by $^1J_{\text{CH}}$.

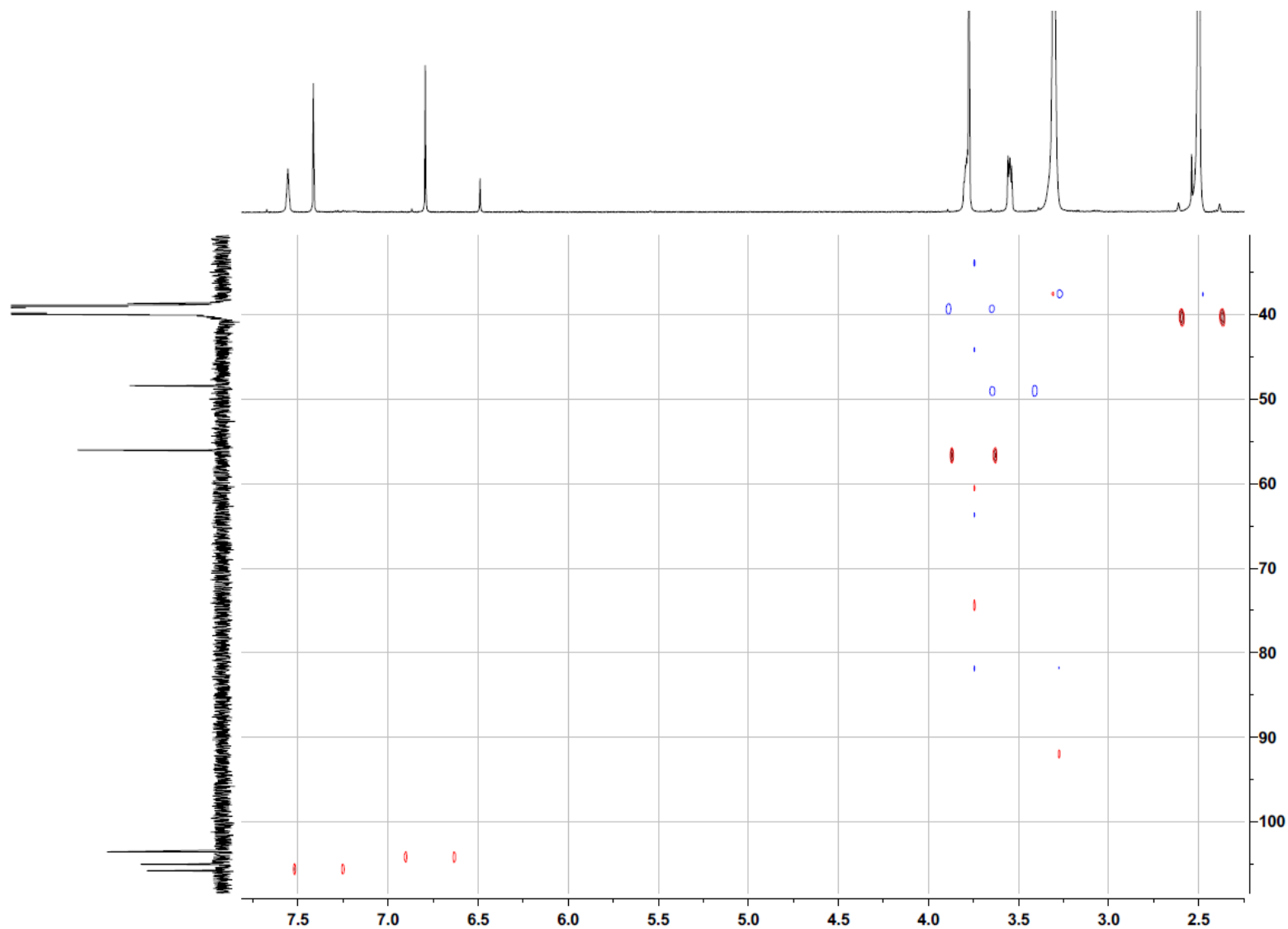


Figure S8. ^1H - ^{13}C HMBC NMR spectrum of naturally-occurring ietrochotazine A (**1**) in $[\text{D}_6]\text{DMSO}$

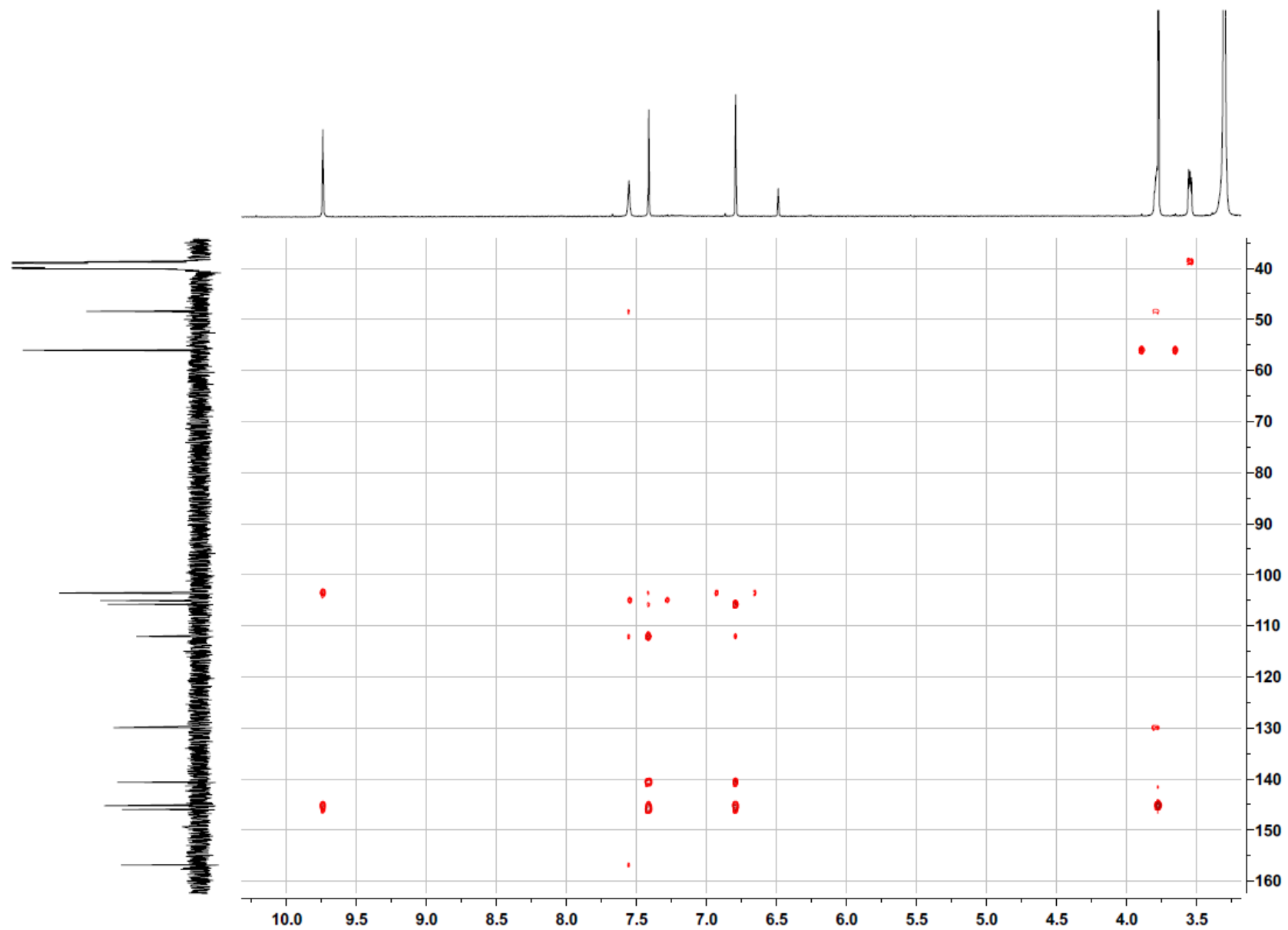


Figure S9. ^1H NMR spectrum of iotrochotadine A trifluoroacetate salt (**2**) in $[\text{D}_6]\text{DMSO}$

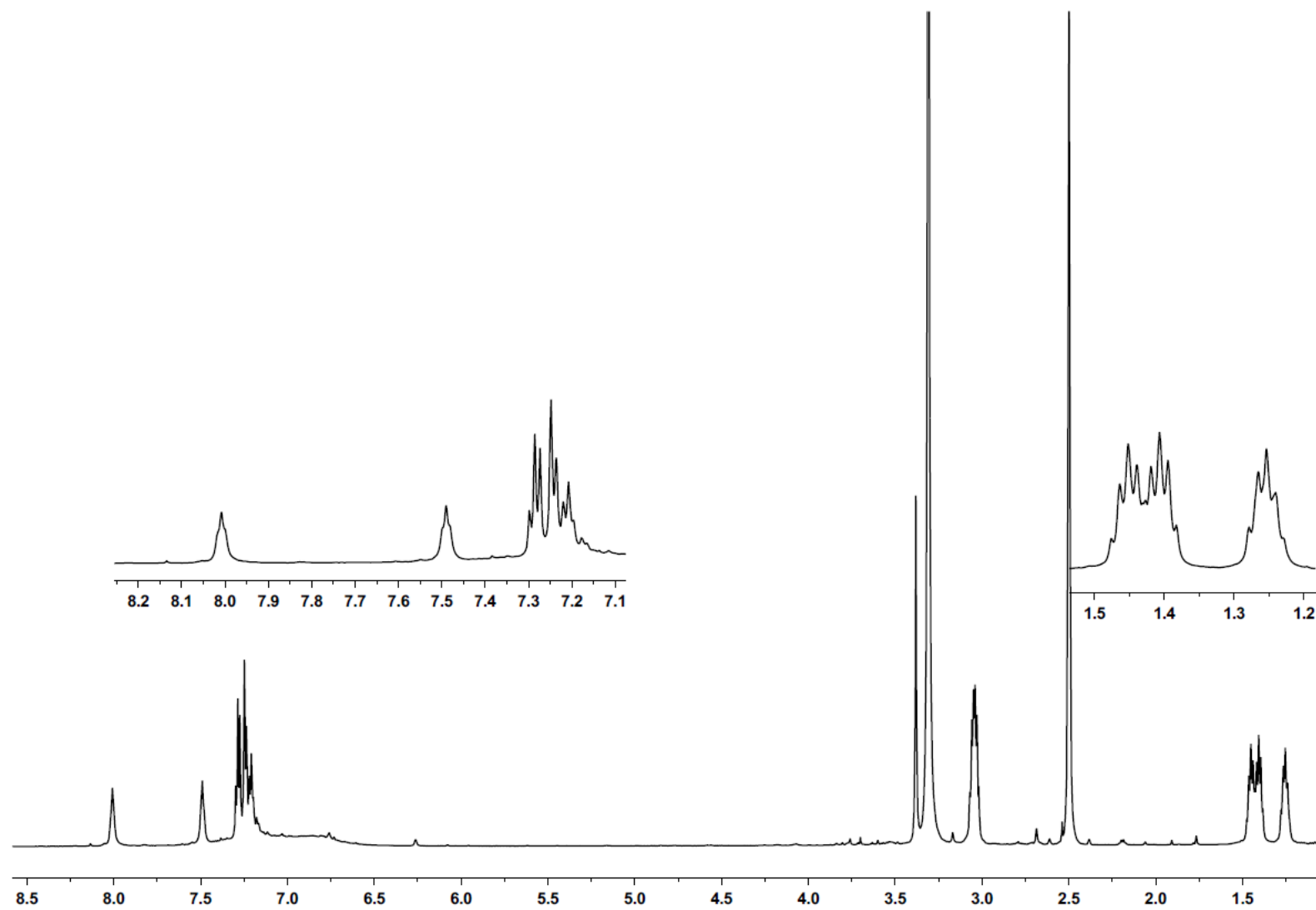


Figure S10. ^{13}C NMR spectrum of iotrochotadine A trifluoroacetate salt (**2**) in $[\text{D}_6]\text{DMSO}$

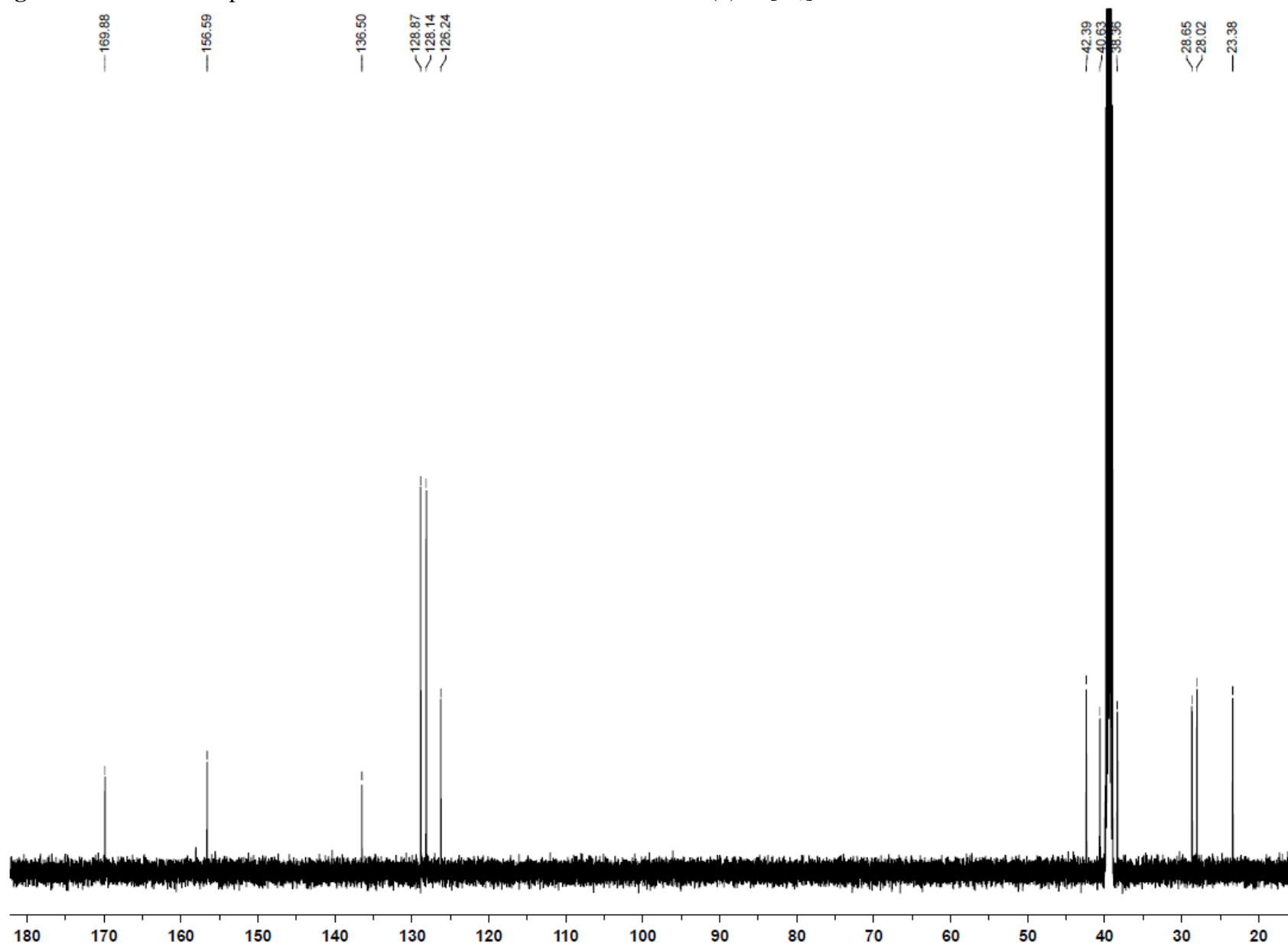


Figure S11. Edited ^1H - ^{13}C HSQC NMR spectrum of iotrochotadine A trifluoroacetate salt (**2**) in $[\text{D}_6]\text{DMSO}$. The decoupler was turned off during acquisition resulting in signals being split by $^1J_{\text{CH}}$.

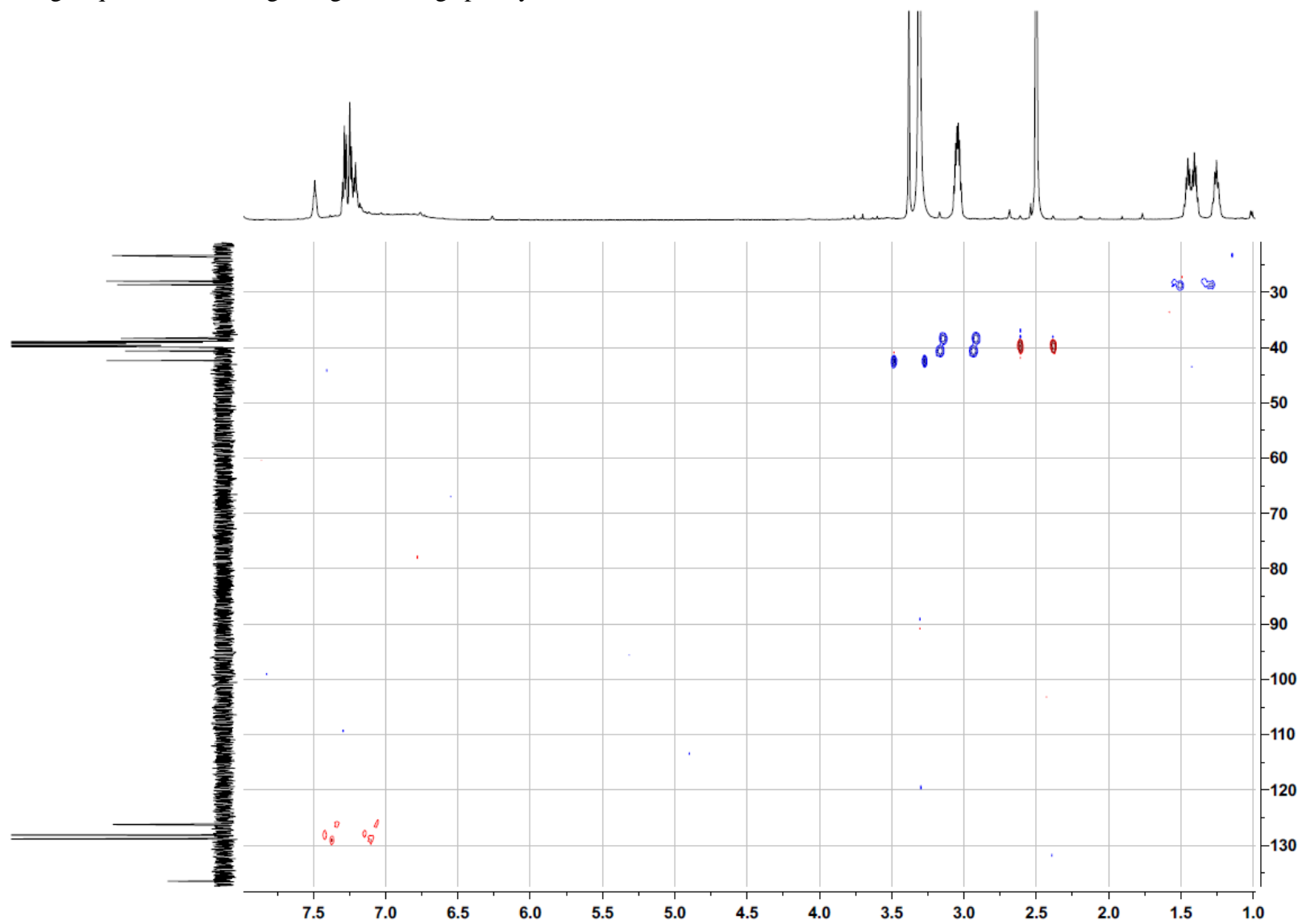


Figure S12. ^1H - ^{13}C HMBC NMR spectrum of iotrochotadine A trifluoroacetate salt (**2**) in $[\text{D}_6]\text{DMSO}$

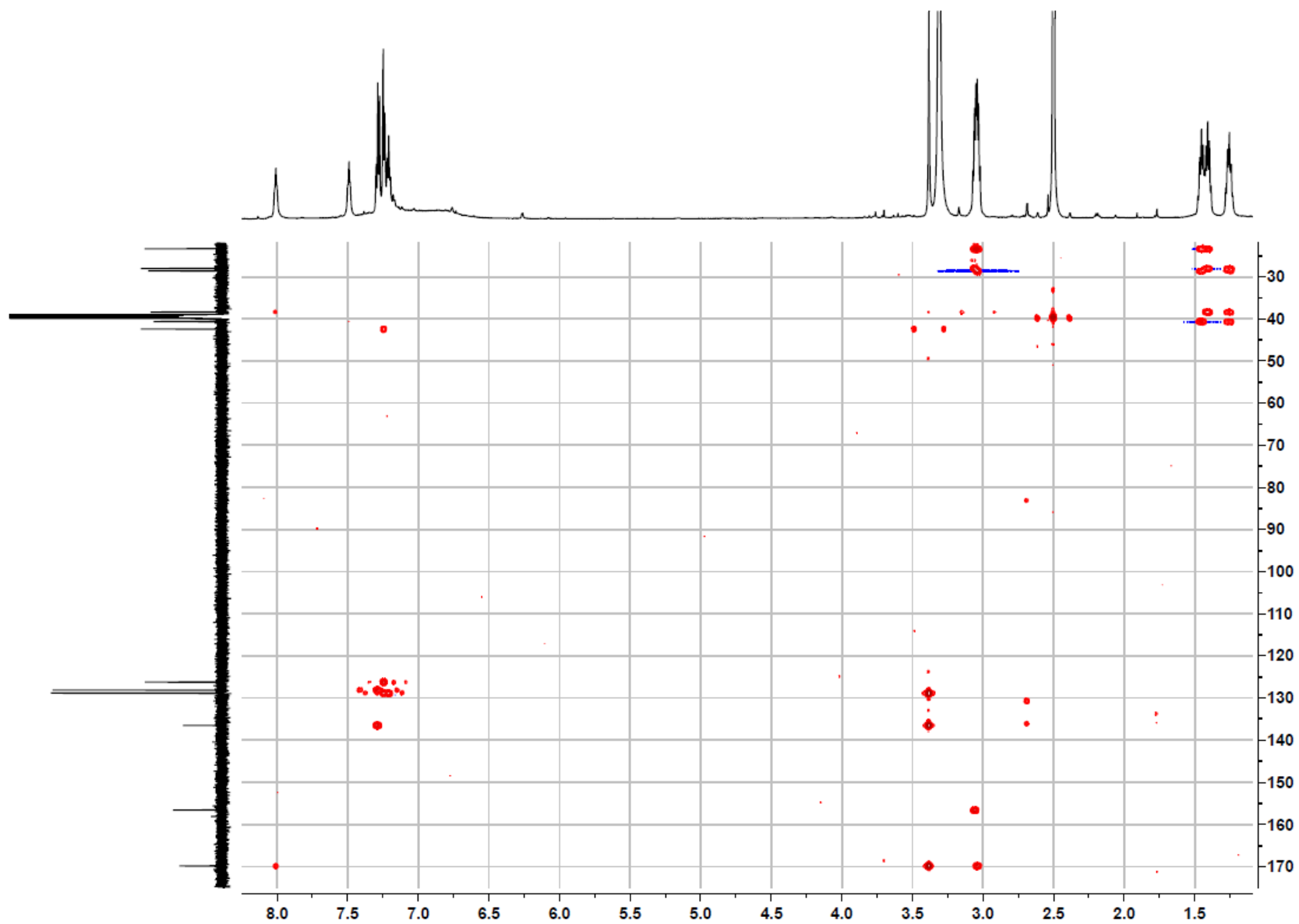


Figure S13. ^1H NMR spectrum of iotrochotadine B trifluoroacetate salt (**3**) in $[\text{D}_6]\text{DMSO}$

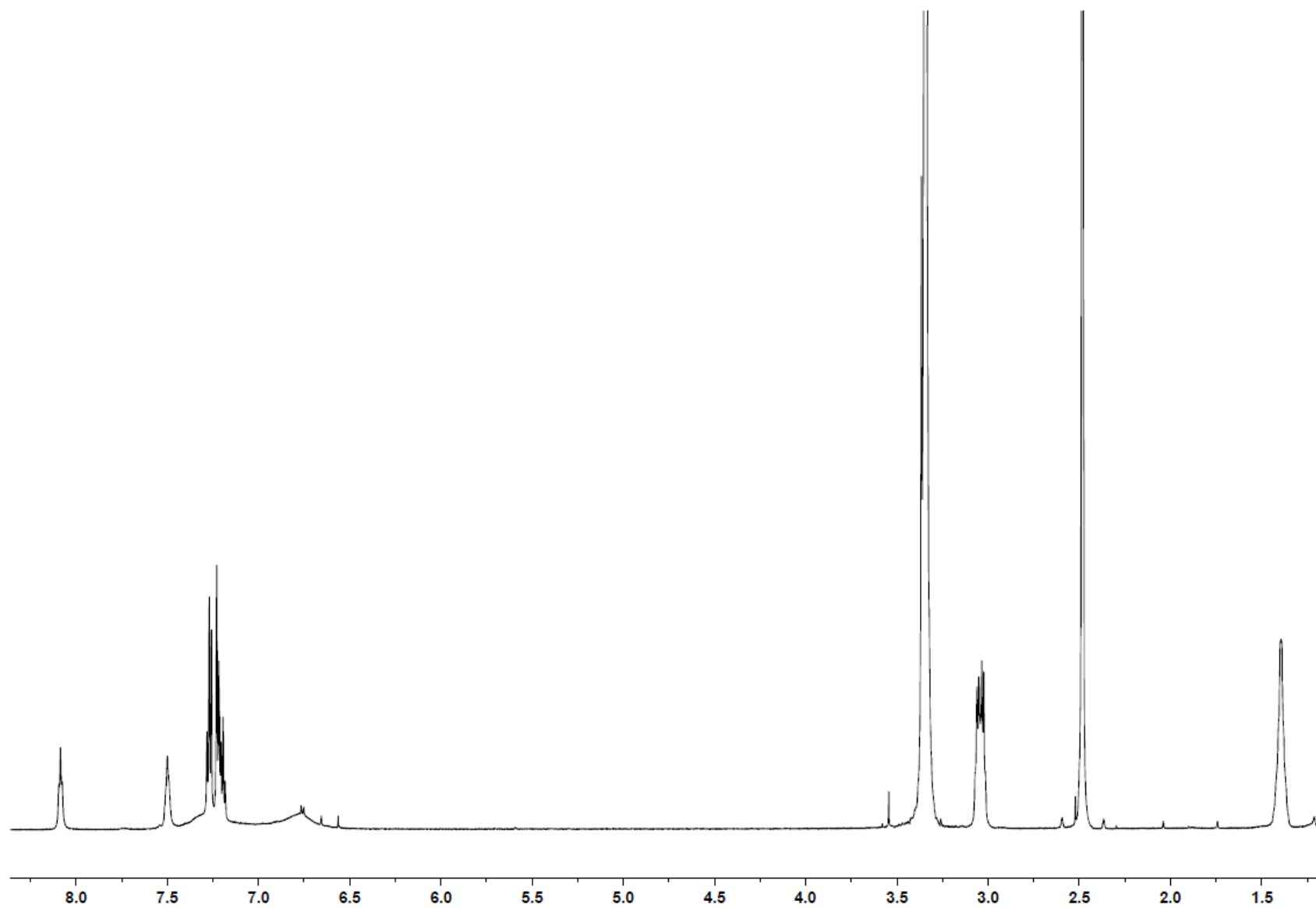


Figure S14. ^{13}C NMR spectrum of iotrochotadine B trifluoroacetate salt (**3**) in $[\text{D}_6]\text{DMSO}$

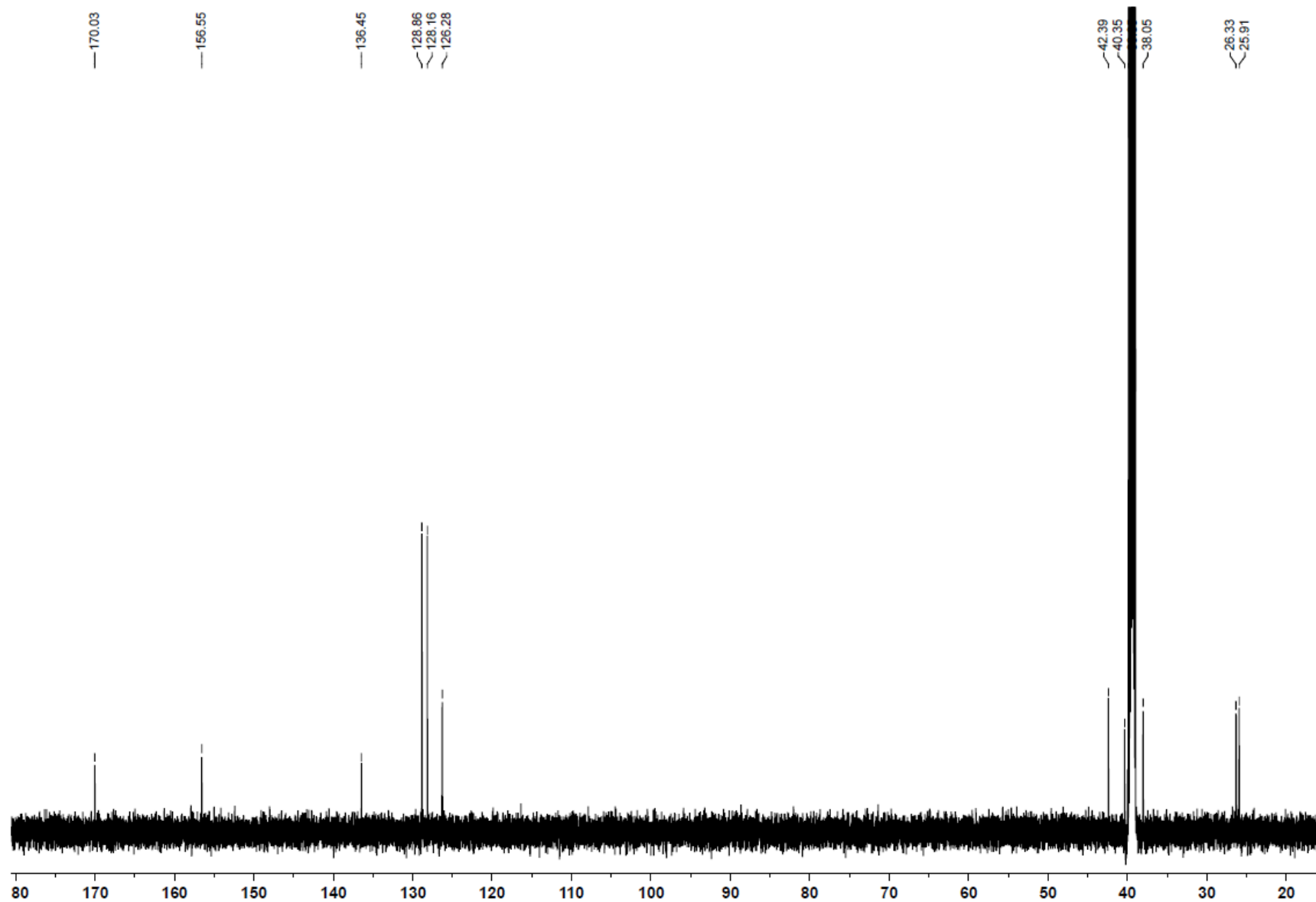


Figure S15. ^1H NMR spectrum of iotrochotadine C trifluoroacetate salt (**4**) in $[\text{D}_6]\text{DMSO}$

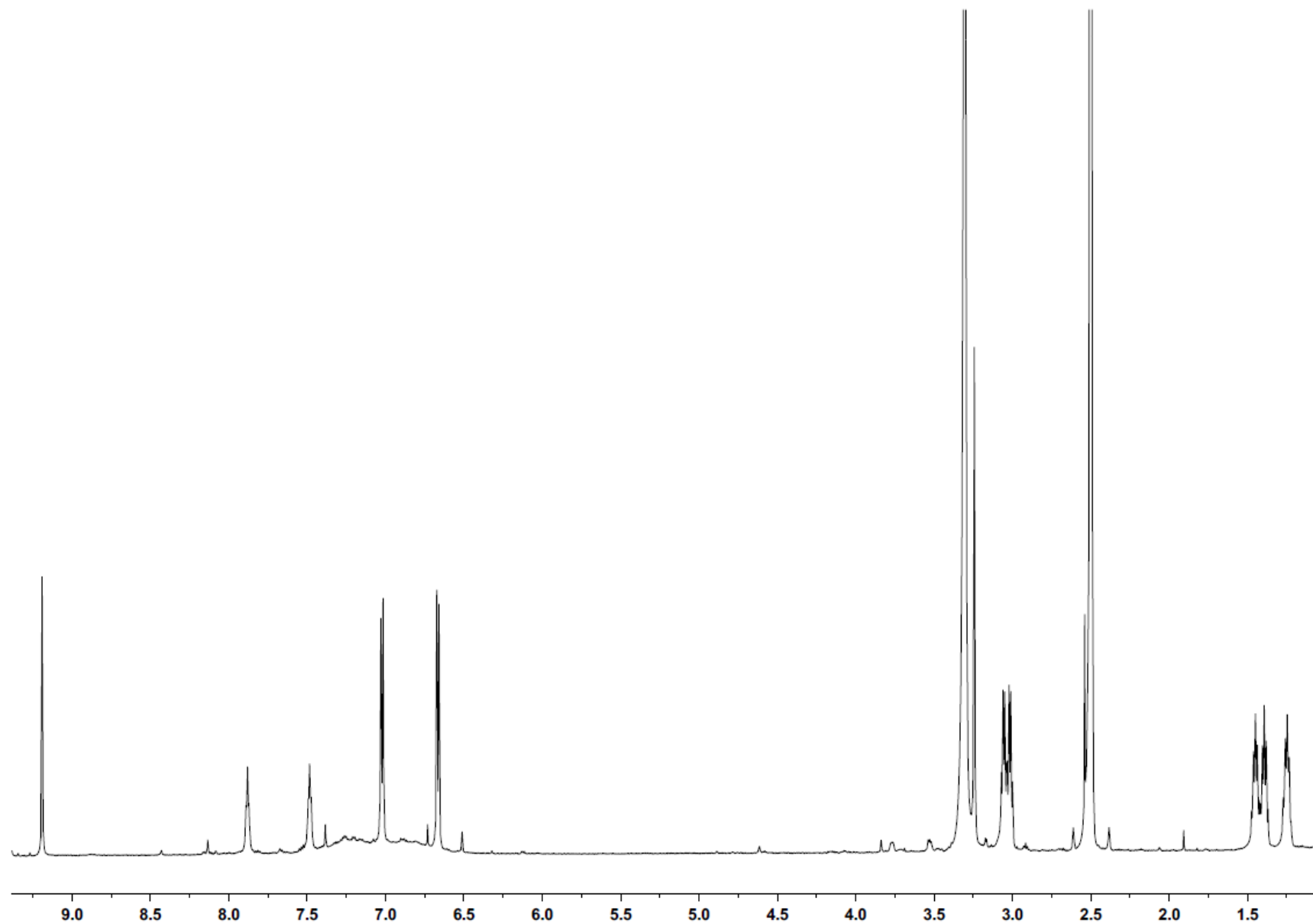


Figure S16. ^{13}C NMR spectrum of iotrochotadine C trifluoroacetate salt (**4**) in $[\text{D}_6]\text{DMSO}$

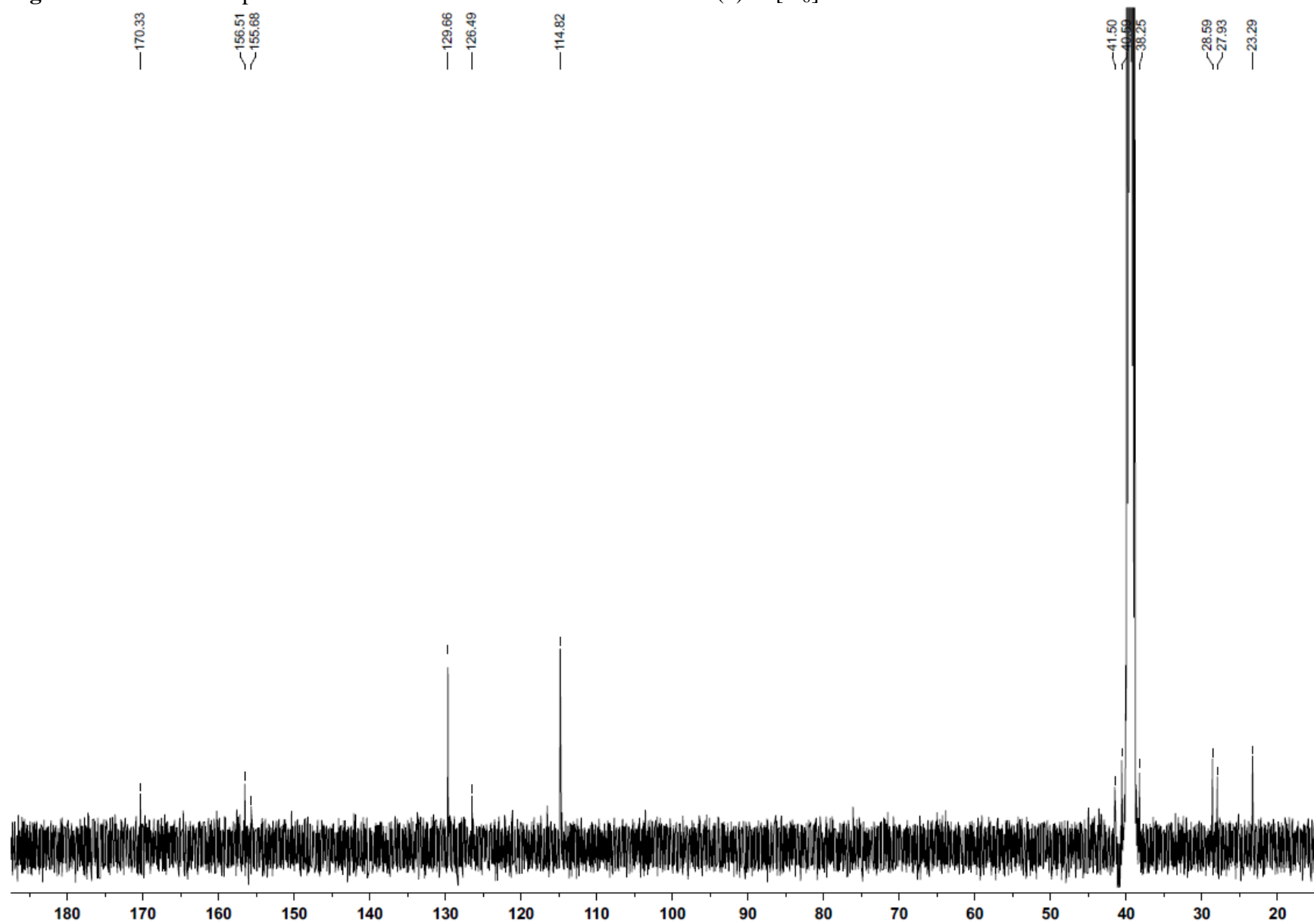


Figure S17. ^1H NMR spectrum of iotrochotadine D trifluoroacetate salt (**5**) in $[\text{D}_6]\text{DMSO}$

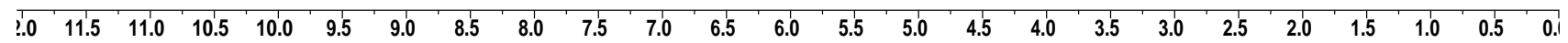


Figure S18. Edited ^1H - ^{13}C HSQC NMR spectrum of iotrochotadine D trifluoroacetate salt (**5**) in $[\text{D}_6]\text{DMSO}$. The decoupler was turned off during acquisition resulting in signals being split by $^1\text{J}_{\text{CH}}$.

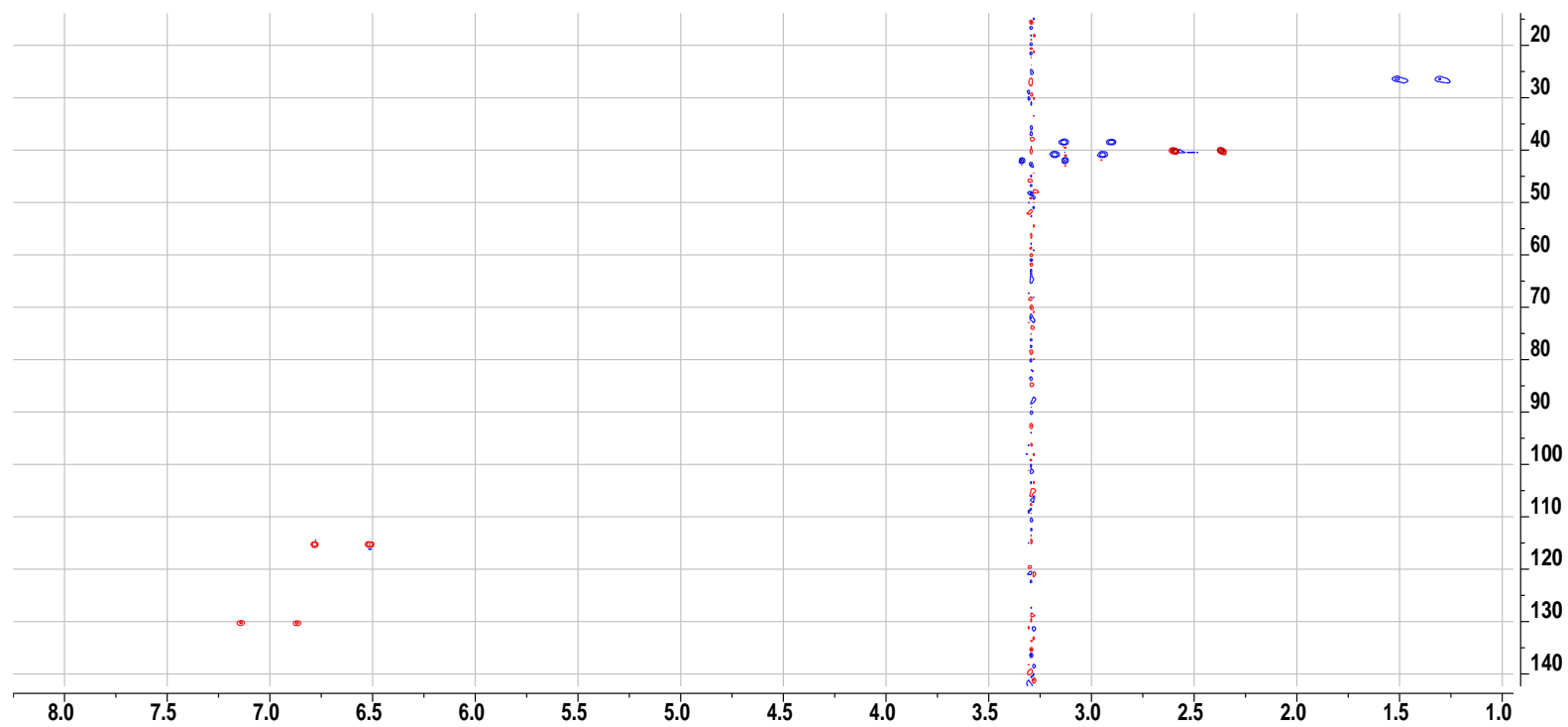


Figure S19. ^1H - ^{13}C HMBC NMR spectrum of iotrochotadine D trifluoroacetate salt (**5**) in $[\text{D}_6]\text{DMSO}$

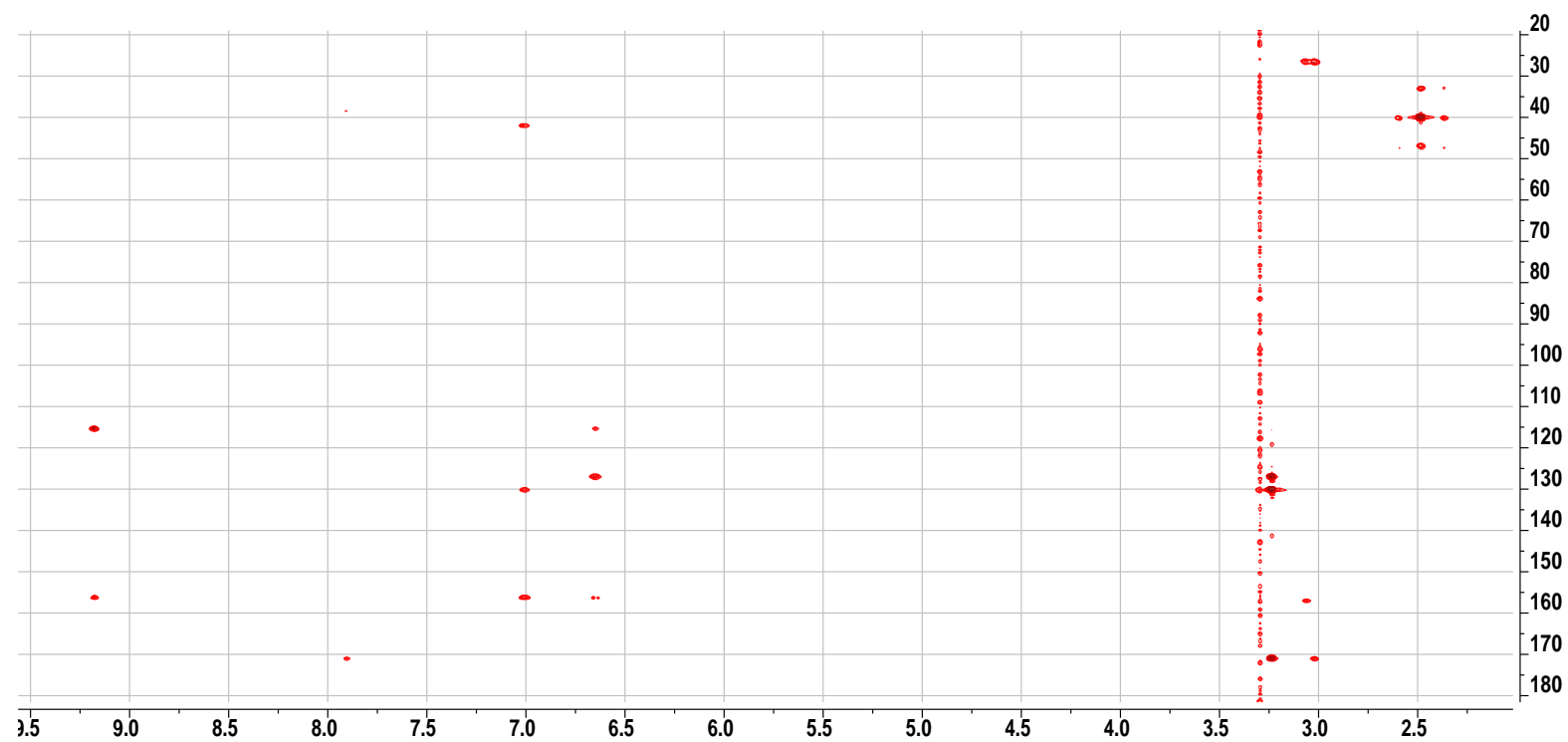


Figure S20. ^1H NMR spectral comparison of naturally-occurring **1** (top spectrum in red) and synthetic **1** (bottom spectrum in blue) in $[\text{D}_6]\text{DMSO}$

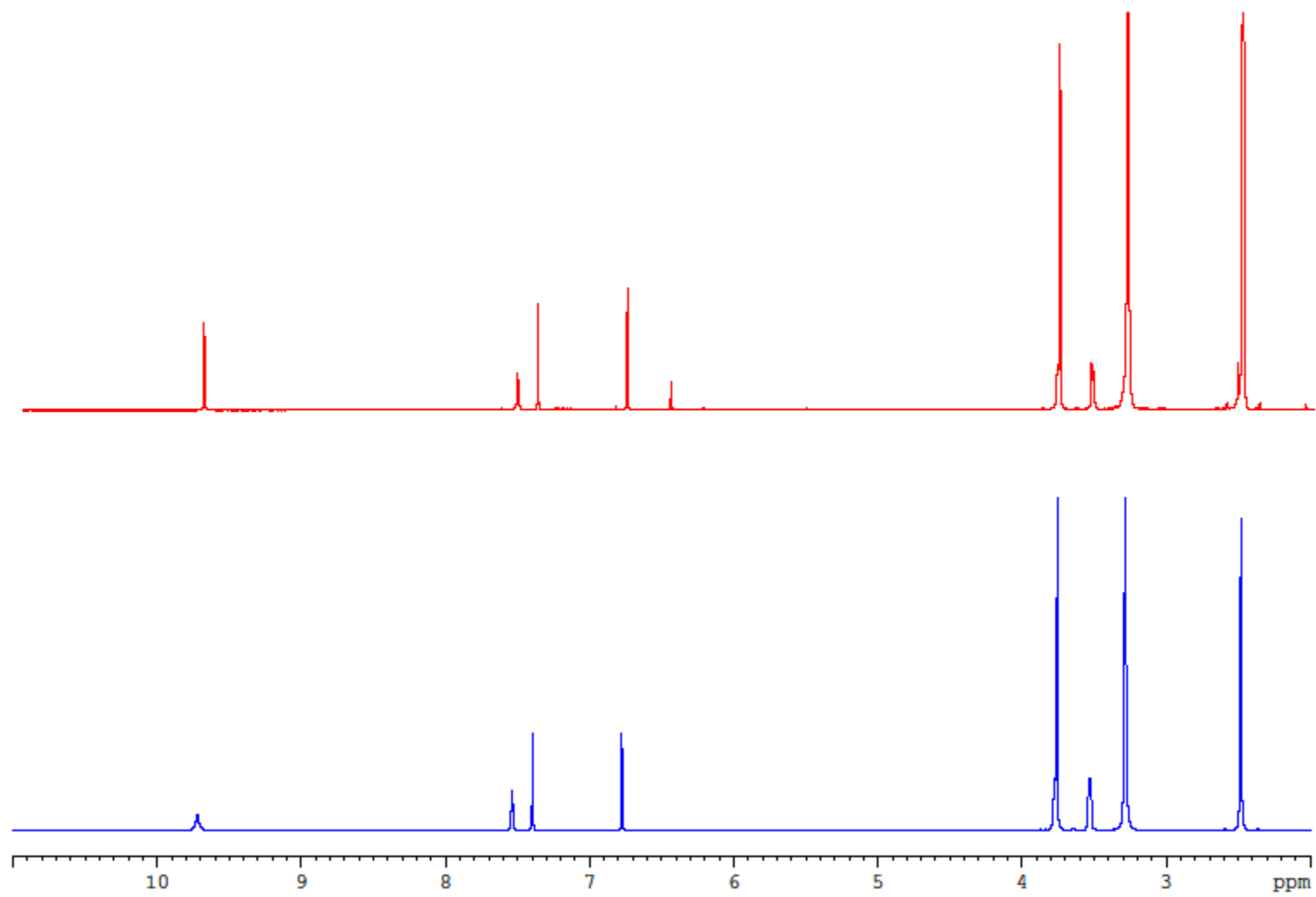


Figure S21. ^{13}C NMR spectral comparison of naturally-occurring **1** (top spectrum in red) and synthetic **1** (bottom spectrum in blue) in $[\text{D}_6]\text{DMSO}$

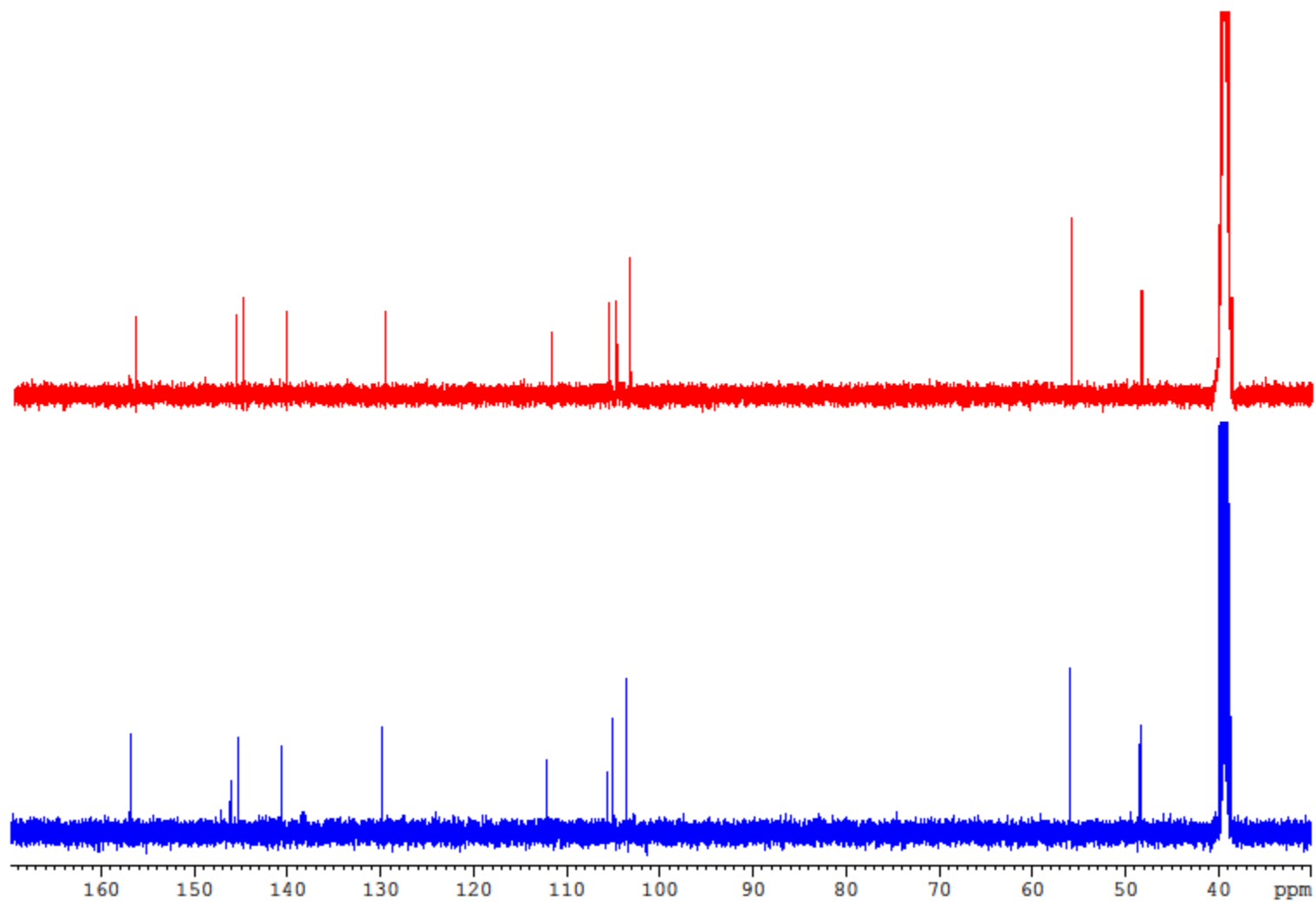


Figure S22. Pototograph of the sponge *Iotrochota* sp. QM2256



References:

1. D. Camp, R. A. Davis, M. Campitelli, J. Ebdon, R. J. Quinn, *J. Nat. Prod.* **2012**, 75, 72-81.
2. J. Demyttenaere, K. Van Syngel, A. P. Markusse, S. Vervisch, S. Debenedetti, N. De Kimpe, *Tetrahedron*, **2002**, 58, 2163-2166.
3. Aihara, K.; Higuchi, T.; Hirobe, M., *Biochem. Biophys. Res. Commun.* **1990**, 168, 169-175.
4. Buchanan, M., S., Carroll, A., R., Wessling, D., Jobling, M., Avery, V., M., Davis, R., A., Feng, Y., Hooper, J., N., A., Quinn, R., *J. Nat. Prod.* **2009**, 72, 973-975.
5. Houssen, W., E., Jaspars, M. *J. Nat. Prod.* **2005**, 68, 453-455.
6. Saifah, E., Suttisri, R., Shamsub, S., Pengsuparp, T., Lipipun, V. *Phytochemistry*, **1999**, 52, 1085-1088.
7. Greger, H., Pacher, T., Vajrodaya, S., Bacher, M., Hofer, O. *J. Nat. Prod.* **2000**, 63, 616-620.